Encounter-Based Density Approximation Using Multi-step and Quantum-Inspired Random Walks

Robert S. Wezeman[1(✉)], Niels M. P. Neumann[1], Frank Phillipson[1,2], and Robert E. Kooij[1,3]

[1] Department of Cyber Security & Robustness, The Netherlands Organisation for Applied Scientific Research, The Hague, The Netherlands
robert.wezeman@tno.nl

[2] School of Business and Economics, Maastricht University, Maastricht, The Netherlands

[3] Faculty of Electrical Engineering, Mathematics and Computer Science, Delft University of Technology, Delft, The Netherlands

Abstract. In this paper we study encounter-based density estimation using different random walks and analyse the effects of the step-size on the convergence of the density approximation. Furthermore, we analyse different types of random walks, namely, a uniform random walk, with every position equally likely to be visited next, a classical random walk and a quantum-inspired random walk, where the probability distribution for the next state is sampled from a quantum random walk. We find that walks with additional steps lead to faster convergence, but that the type of step, quantum-inspired or classical, has only a marginal effect.

Keywords: Agent based Modeling · Population Density Estimation · Quantum Random Walk

1 Introduction

Agent-based modelling (ABM) is a stochastic simulation modeling technique that can be used to study macroscopic properties of complex systems by using microscopic descriptions of individual agents. In ABM, a certain behaviour is modeled by multiple autonomous decision-making entities known as agents. Each agent is given a set of rules that describe how the agent should behave and interact with the environment. Models based on agents with very simplistic individual behaviour can be used to study systems with complex interactions. ABM has a wide range of applications, such as predicting customer flows or predicting congestion and flows in network-traffic [4]. Even certain aspects of the stock-markets can be modelled by agent-based models. Furthermore, ABM can be used to model organizational design and operational risk in organizations, but also the adoption and innovation dynamics [4]. More recently, ABM models have

K. Arai (Ed.): SAI 2023, LNNS 711, pp. 517–531, 2023.
https://doi.org/10.1007/978-3-031-37717-4_32

been applied for online recommendation systems [10] and in simulations for the energy management in IoT surveillance systems [5].

The work by Musco, Su, and Lynch[11] on density estimation using random walks is the starting point for this work. In their work, ants serve the role as anonymous agents and are placed on a two-dimensional grid. Each ant has the task to give an estimate of the density of other ants on the grid, i.e., the total number of other ants divided by the grid size.

It was shown, with first work already in the 90s, that ants use knowledge of the number of other ants in their surrounding to make strategical decisions. For example when to relocate [12], whether to engage with or retreat from an enemy colony [1], or how to allocate tasks in the nest [8,13]. Gordon, Paul, and Thorpe [9] showed that ants appear to use encounter patterns to cue the density of nestmates. Inspired by these biological phenomena, Musco et al. created an ABM in which randomly walking agents are assumed to be able to track the number of collisions with other agents over time. With this assumption, agents can give a fairly accurate estimate for the agent density on the grid based on the collision rate. Furthermore, the authors give theoretical bounds on the proximity of the estimated density $\tilde{d}$ to the true density d, depending on two type of random walks, a classical random walk or a connected random walk.

In a connected random walk agents can move to an arbitrary grid point at each time step. The total number of collisions an agent encounters can be modeled for this type of random walk by sampling from independent Bernoulli trials with success probability d for each agent. Using a Chernoff bound it can be shown that, within $\mathcal{O}\left(\frac{\log(1/\delta)}{d\epsilon^2}\right)$ rounds, the encounter rate $\tilde{d}$ approximates the true density d with probability $P\left(\left|d-\tilde{d}\right| \leq \epsilon\right) > 1-\delta$ [11].

In a classical random walk, agents are only allowed to jump to directly adjacent grid points at each time step. The analysis for this case is therefore also more complex. Agents that initially start close to each other, are likely to collide repeatedly in near future rounds. On average, compared to the connected random walk, agents have more collisions with less agents.

We call a random walk *fast mixing* if the location of agents only weakly correlates with its previous location. An excellent example of such a random walk is the connected random walk, where there is no correlation at all between the locations at different time steps. On the other hand, we call a random walk *slow mixing* if the location of agents correlates strongly between different rounds. The classical random walk is an example of a slow mixing random walk. The encounter-rate-based density estimation using a classical random walk is nearly as accurate as the fully connected random walk, as shown by Musco et al. For the classical random walk, after $\mathcal{O}\left(\frac{\log(1/\delta)}{d\epsilon^2} \cdot (\log\log(1/\delta) + \log(1/d\epsilon))^2\right)$ rounds, the encounter rate $\tilde{d}$ approximates the true density d with probability $P\left(\left|d-\tilde{d}\right| \leq \epsilon\right) > 1-\delta$. This differs from the fully connected estimate only by a multiplicative factor $(\log\log(1/\delta) + \log(1/d\epsilon))^2$.

We extend this work by considering different types of random walks that allow each agent to move to grid points other than the directly adjacent ones in each time step. We consider different underlying distributions for random walks, including a uniform distribution and a distribution inspired by a quantum random walk. Note, Musco et al. only allow for the number of rounds to be smaller than the total grid size. We use simulations with more rounds than the total grid size to show that the encounter-rate-based density estimation converges faster for random walks with a wider spread in the probability distribution.

We first give a formal problem description including an algorithm to run the encounter-based density estimation for different type of random walks in Sect. 2. In Sect. 3 we show our simulation results for different types of random walks and in Sect. 4 we give our conclusions. In Appendix A we formalize the concept of a quantum random walk in two-dimensions and show how we obtain the used quantum-inspired random walk distribution.

2 Problem Formulation

We consider the same situation as described by Musco et al., that is, we consider a square two-dimensional grid consisting of A nodes. Each node is described by its coordinates (x, y) with $0 \leq x, y < \sqrt{A}$. To prevent ourselves from having to deal with possible complicating boundary issues we connect the opposite edges of the grid with each other, which results in a torus.

As the initial situation we place $N + 1$ agents uniformly at random on this two-dimensional torus. The position of each agent is described by the (x, y) coordinates of the node on the grid. In this model, it is possible that multiple agents occupy the same node and hence have the same (x, y) coordinates, as illustrated in Fig. 1. Here $Count(i, j) = k$ means that there are $k + 1$ agents located at the node with coordinates $(x, y) = (i, j)$.

From the perspective of a single agent, the density d of other agents on the grid is given by the total number of other agents divided by the number of possible nodes these agents can occupy, $d = \frac{N}{A}$. The agent now tries to estimate this density by performing a random walk, and keeping track of the amount of collisions with other agents. Intuitively, it makes sense that the rate at which collisions occur is related to the density. On average, if you collide with other agents often, it is likely that the density is high.

We model the behaviour of the agents by letting them take steps in successive rounds. In each round, all agents take a random step, according to some probability distribution P_{step}. Each agent then counts the number of other agents their grid point of that round. After t rounds, each agent can estimate the density d by $\tilde{d} = \frac{c_t}{t}$, with c_t the total number of collisions observed in the t rounds. Note that the agents are modeled to be memoryless except for the total number of collisions. The full routine for each agent is captured in Algorithm 1.

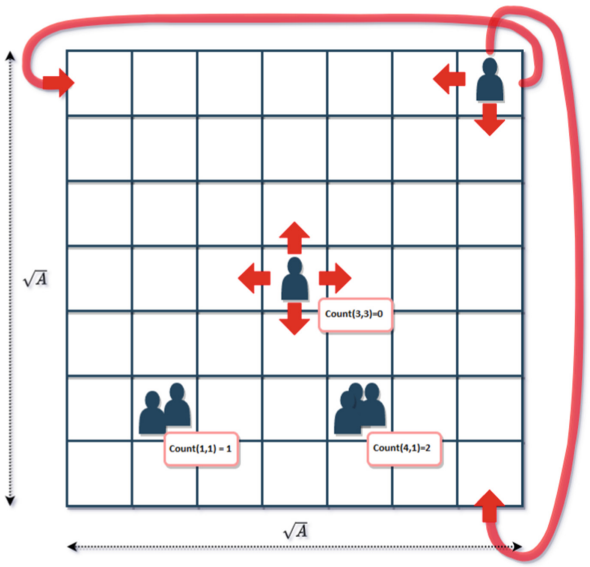

Fig. 1. Schematic Overview of the Grid with Different Agents Located in it, from [11]

Algorithm 1. Random-Walk-Based Density Estimation

```
c := 0;
for i=1...t do
    step := generateRandomStep()          ▷ Sample a step from P_step
    position := position + step
    c := c + count(position)              ▷ Update collision count
end for
return d̃ = c/t
```

Algorithm 1 introduces two functions. The first, *generateRandomStep*(), samples a random step from a probability distribution P_{step}; The second, *count* (*position*), counts all *other* agents currently located at the specified *position*. This function can be used to update the collision count.

We consider three different types of random walks, a uniform-, a classical- and a quantum-inspired random walk as primer for the probability distribution P_{step}. Let a step that an agent can take from node (x_1, y_1) to node (x_2, y_2) be described by the x- and y-displacement. For each random walk, we let $\mathcal{U}$ denote the set of all possible steps an agent can take. We define the three considered random walks as follows

1. **Uniform random walk:** All possible steps in $\mathcal{U}$ are equally likely, i.e., $P^{\mathcal{U}}_{step}(X) = \frac{1}{|\mathcal{U}|}$ for all steps X in $\mathcal{U}$. We let $\mathcal{U}$ be the set of all steps that have a combined x- and y- displacement less than or equal to a given integer M. The corresponding random walk will be denoted by *Uniform M*. The

possible steps $\mathcal{U}$ for a uniform random walk with $M = 1$ are given by

$$\mathcal{U}_1 = \{(1,0), (-1,0), (0,1), (0,-1), (0,0)\}.$$

The case when M is sufficiently large, such that $\mathcal{U}$ contains all the steps to all possible nodes, is sometimes referred to as the connected random walk, as in that case agents effectively traverse a fully connected graph. In the following figures we will refer to this case as *Connected*.

2. **Classical random walk:** Also for this case we consider $\mathcal{U}$ to be the set of all steps that have a combined x- and y- displacement less than or equal to a given integer M, but now the probability is not uniform, but given by

$$P^M_{step}(X) = C_M(X) \left(\frac{1}{5}\right)^M,$$

where $C_M(X)$ is the number of different routes from the starting point to X in M steps from $\mathcal{U}_1$. The corresponding random walk is denoted by *Classical M*, which is the result of M consecutive single classical random walks.

3. **Quantum(-inspired) random walk:** Similar to the classical random walk, however, the probability distribution is now obtained from a two-dimensional quantum random walk with a maximum displacement M. We denote the resulting random walk by *Quantum M* Due to the inherent interference property, quantum random walks tend to have a wider spread, with the expected distance from the start after M random steps being linear in M, or $\Omega(M)$ for short. This is different for the earlier discussed classical random walk with maximum displacement M, for which the spread is similar to the square root of M, or $\mathcal{O}(\sqrt{M})$. We take a weighted sum of four different quantum random walks such that the final probability distribution becomes symmetric. The obtained distribution has a high probability to stay close at its current position while simultaneously also having a relative large probability to make a large step, see Fig. 2d. In Appendix A background information on quantum random walks is given together with the precise construction that we used to create the quantum-inspired probability distribution.

In Fig. 2, the probability distributions are plotted for the different random walks. We remark that the probability distribution of the quantum-inspired random walk appears to create a chess board pattern. This corresponds to what one would expect if in each step, the agent has to move and is not allowed to remain at the current position. For an M-step quantum random walk, with M being even (odd), the probability to end up an odd (even) number of places away is zero. As a consequence, agents, that are initialized an odd number of steps away from each other, can never collide using our quantum-inspired random walks. This effectively halves the grid size. We deal with this issue by separating the agents in two groups. Each group is placed randomly on the grid, however in such a manner that agents within the same group are always an even number of steps separated from each other while agents from different groups are always an odd number of steps separated. This problem does not occur for the uniform-

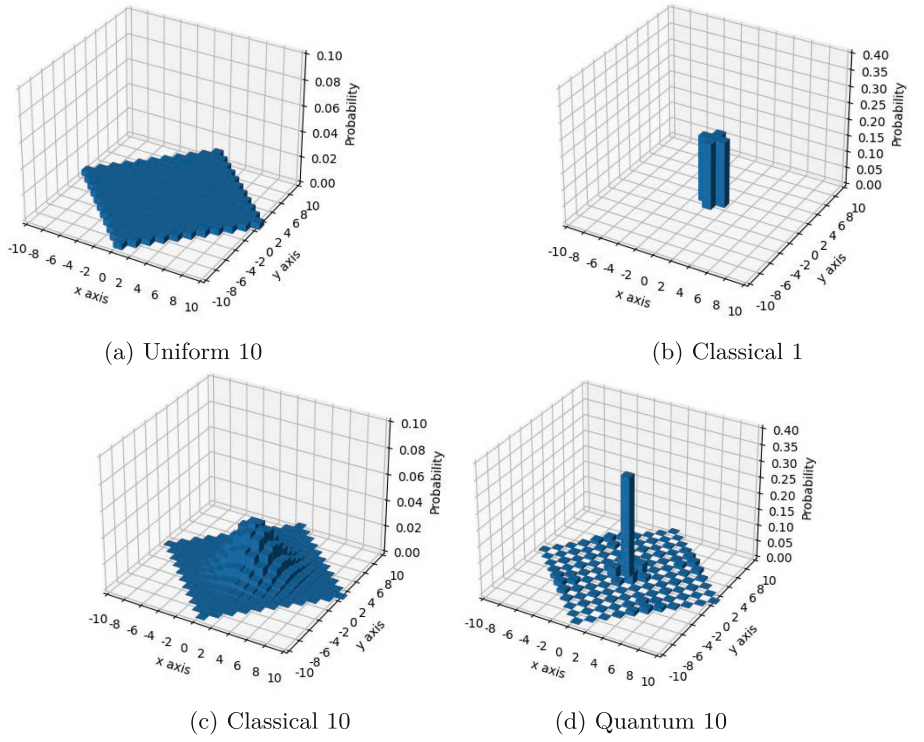

(a) Uniform 10 (b) Classical 1

(c) Classical 10 (d) Quantum 10

Fig. 2. Probability Distributions for Different Type of Random Walks and Different Values of Maximum Displacement M per Step (1 or 10)

and classical random walk because we have included the possibility for an agent to stand still in our definition of these walks, $(0, 0) \in \mathcal{U}$.

Encounter-based density estimation using different types of random walks can never outperform the connected random walk in terms of how fast the estimate converges to the true value d: In the connected random walk, in each round on average exactly d collisions occur, independent of the previous rounds. This argument does not hold for the other random walks. The number of collisions in each rounds is correlated with the positions of all agents before taking a step. Depending on whether agents can or can not reach each other within one time step, the average number of collisions for that time step will be higher or lower than d. As a consequence the average number of collisions d can only be reached over multiple time rounds, resulting in more variance and thus slower convergence of the density estimation. With this knowledge, we can compare different types of random walks with the connected random walk as a baseline.

Our approach simulates agents performing Algorithm 1 for different types of random walks on different grid sizes. We compare the error of the density estimation of agents with respect to the number of steps taken by the agents.

3 Results

As described in the previous section, we ran multiple simulations of Algorithm 1 for different grid sizes and different types of random walks. For each grid size and type of random walk, we will simulate multiple independent instances. In each instance, all $N + 1$ agents will independently produce a density estimate.

For our simulations, we considered 1,000 instances for each grid size and type of random walk combination. Furthermore, we have fixed $N = 26$ in all simulations. We compare the density estimation of different random walks on the first 100,000 random walk rounds. In Fig. 3 the encounter-based density estimation is shown for each individual agent on a 10×10 grid for the first 20,000 steps. In this example, the true density of agents on the grid is given by $d = \frac{N}{A} = \frac{25}{100}$. As a performance metric we define the average absolute relative error after t rounds by the sum of the absolute errors averaged over the agents and the instances, relative to the true density d:

$$Err(t) = \frac{1}{1000} \sum_{j=1}^{1000} \left| \left(\frac{1}{26} \sum_{i=1}^{26} \frac{\tilde{d}_{i,j}(t) - d}{d} \right) \right|,$$

where $\tilde{d}_{i,j}(t)$ is the encounter-based density estimation for agent i in instance j after t rounds. Alternative metrics are also possible, for example by averaging the density estimation error of each individual agent instead of averaging over all agents in one instance. The disadvantage of that metric is however that it fluctuates more and thus takes more instances before randomness is suppressed and hence more simulation time is required. The global convergence behaviour in which we are interested, how different random walks with different step sizes on different grid sizes compare to each other, is not affected by the chosen metric.

In Fig. 4 the average absolute relative error is shown for the uniform, classical and quantum-inspired random walk with *different step sizes* on a 80×80 grid. For each type of random walk, we observe that the encounter-based density estimation converges faster for larger step size.

In Fig. 5 the connected and uniform random walk are compared for various grid sizes and number of steps. We see that the 5-step uniform random walk on a 40×40 grid, the blue line, performs almost as good as the connected random walk shown in grey. On a larger 80×80 grid, the 5-step uniform random walk does not perform nearly as well as before. Increasing the number of simultaneous steps taken by the random walk from 5 to 10, appears to result in similar performance as a connected random walk. This is as expected, as by increasing the grid and number of steps by the same factor, the same percentage of the total grid can still be covered in a single random step. As a consequence, a collision is possible with the same percentage of other agents. The probability of this is however smaller, as there are more locations. Similarly, the density is also smaller. The same pattern can also be observed for the two other types of random walks.

The type of random walk affects the speed at which the encounter-based density estimation converges to d, as shown in Fig. 6. The uniform random walk

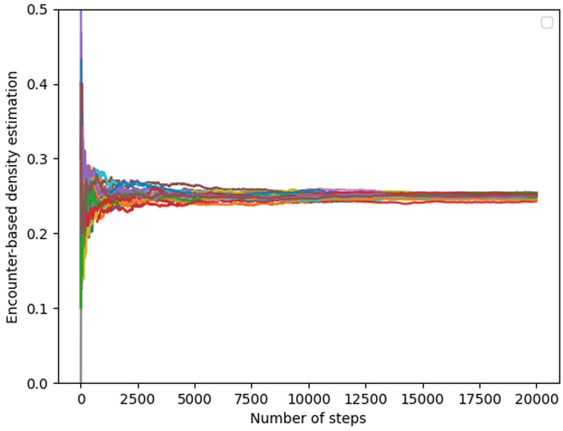

Fig. 3. Encounter-Based Density Estimation for each of the 26 Agents on a 10×10 that are each Performing a Classical Random Walk. The True Density from the Perspective of each Agent is $d = 0.25$

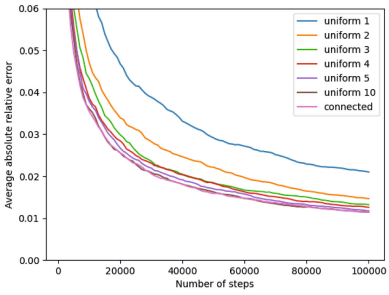

(a) Uniform Random Walk

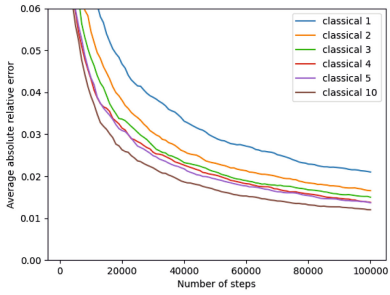

(b) Classical Random Walk

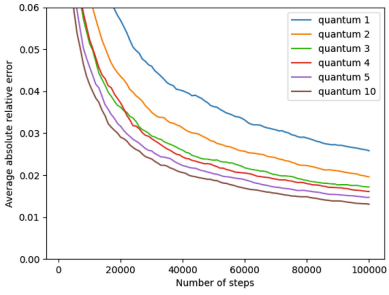

(c) Quantum-Inspired Random Walk

Fig. 4. Average Absolute Relative Error for Uniform, Classical and Quantum-Inspired Random Walks for Different Step Sizes on a 80×80 Grid

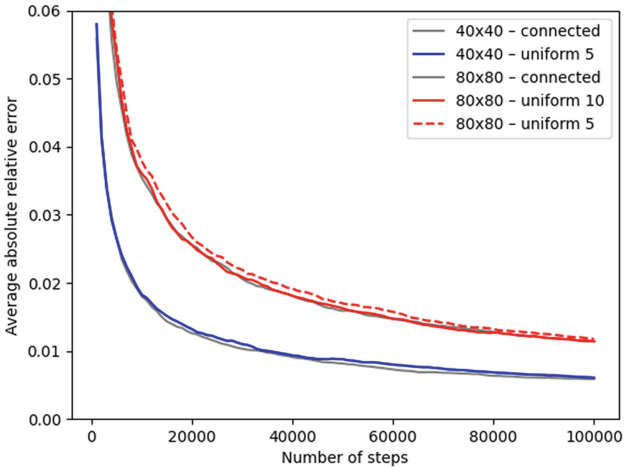

Fig. 5. Average Absolute Relative Error for the Uniform Random Walk and the Connected Random Walk, for Different Grid Sizes and Number of Steps

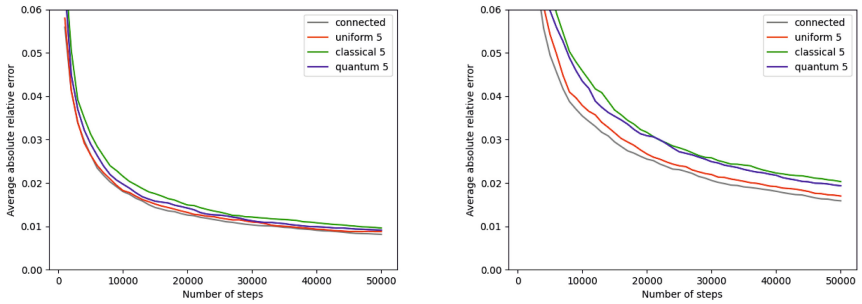

(a) Grid 40×40 (b) Grid 80×80

Fig. 6. Average Absolute Relative Error for Different Type of Random Walks for Different Grid Sizes

converges slightly faster to the true density than the quantum-inspired random walk followed by the classical random walk. A possible explanation for this is that distributions with a wider spread allow for more collisions between agents that are initially farther apart. These distributions also have a smaller chance of a quick re-collision, once a collision between two agents has occurred.

4 Conclusions

We extended the work by Musco et al. by considering different types of random walks and allowing for more steps to be taken. Their contribution is based on theoretical results that show that the encounter-based density estimation gives a good estimate of the true density. In this work we looked at a simulation based

approach and showed for different types of random walks that the encounter-based density estimation converges faster for random walks with larger step size. Furthermore, we showed that the type of random walk affects the rate at which the encounter-based density estimation converges. The distributions that are more likely to result in a wider spread, the uniform- and quantum-inspired random walk, converge faster to the true density of agents on the grid than standard single-step random walks. A possible explanation is that agents located farther away are more likely to collide, while also preventing a high number of re-collisions once they have collided.

An interesting follow-up question is what the effect is of non-uniform initial starting positions of the agents. Similarly, it is interesting to consider the effect of agents traversing a non-regular grid. Another possible direction could be to consider combined effect of different agents performing different types of (random) walks simultaneously.

As further work it is interesting to increase simulation size and apply our work to a more realistic application, for example, simulating energy management in IoT surveilence systems [5]. Another direction our work could be applied in is the field of reinforcement learning, for example, to improve agent based recommendation systems [10].

Appendix

A Quantum Random Walk

A.1 Quantum Walk in One Dimension

A one-dimensional classical random walk is described by an agent that is allowed to move with integer steps on a one dimensional line. The position of the agent after a certain number of rounds can be described by an $n \in \mathbb{Z}$, with respect to its starting position. Each round the agent moves with equal probability to the left on the number line, $n-1$, or to the right, $n+1$. This definitions slightly differs from the one in Sect. 2, as there agents are also allowed to stand still.

In the quantum analogue, the position of a one-dimensional quantum agent is described by the quantum state $|n\rangle$ with $n \in \mathbb{Z}$. The most generic step that an agent in the state $|n\rangle$ can take is given by

$$|n\rangle \rightarrow a\,|n-1\rangle + b\,|n\rangle + c\,|n+1\rangle\,, \tag{1}$$

where the parameters a, b and c can be some complex valued parameters. To guarantee the preservation of total probability, quantum mechanics only allows for unitary operations acting on states. It can now easily be shown that there does not exist a unitary transformation matrix such that two of the parameters a, b and c are non-zero. This means that only trivial movements are allowed, always moving to the left, always staying at the same position or always moving to the right. This problem of only having trivial movement is overcome by using an extra register. This register is in literature often referred to as the *coin* state.

Define the state space as all states $|n\rangle \otimes |c\rangle$ in $\mathbb{Z} \times \text{span}\{|0\rangle, |1\rangle\}$. A quantum random walk is then defined by two successive unitary operations:

1. First apply what is known as the coin-flip operator C

$$C(|n\rangle \otimes |0\rangle) = a|n\rangle \otimes |0\rangle + b|n\rangle \otimes |1\rangle$$
$$C(|n\rangle \otimes |1\rangle) = c|n\rangle \otimes |0\rangle + d|n\rangle \otimes |1\rangle$$

2. Followed by the shift operator S

$$S(|n\rangle \otimes |0\rangle) = |n-1\rangle \otimes |0\rangle$$
$$S(|n\rangle \otimes |1\rangle) = |n+1\rangle \otimes |1\rangle$$

A single step of the quantum walk is given by an application of both operators. There is still freedom in choosing the exact coin operator C. The only restriction is that the corresponding matrix is unitary. A common choice for the coin operator is the Hadamard coin, given by

$$C = \mathbb{I}_2 \otimes H = \mathbb{I}_2 \otimes \frac{1}{\sqrt{2}} \begin{pmatrix} 1 & 1 \\ 1 & -1 \end{pmatrix}.$$

In Fig. 7 the probability distribution of the first three steps for a classical random walk is compared to the probability distribution of a quantum random walk. The quantum walk starts from the initial state $|0\rangle \otimes |1\rangle$ and uses the Hadamard coin as coin operator. The classical random walk starts at the $n = 0$ position. After the first two steps of the random walk, the probability that the agent is found at a certain position is the same for both types. The random walks start to fundamentally differ from each other from the third step onward. The classical random walk keeps spreading symmetrically around the origin, splitting its probability equal to the left and the right. The quantum random walk appears to have a bias to the left and does not split its probability equally in the two directions. This effect is explained by quantum interference effects, where the amplitudes of specific states are cancelled. These differences become even more apparent when more random steps are taken.

Both the coin operator and the initial superposition affect the direction of such a potential drift in the probability distribution. In Fig. 8 the probability distribution after a quantum random walk consisting of 100 steps is shown for the Hadamard coin with different initial superposition. These distributions show different behaviour when compared to the classical expected binomial distribution. The bias in the probability distribution is corrected for by considering a different (symmetric) coin or a different initial starting position. However, two differences between the classical and quantum random walk remain independent of the initial starting position or the used coin.

– After t steps, the position n at which the agent is most likely found is given by $|n| \approx \frac{1}{2}\sqrt{2}t$ for the quantum random walk and $n \approx 0$ for the classical random walk.

– After t steps, the expected distance of the agent away from the initial position is given by $\Omega(t)$ for the quantum random walk and $\mathcal{O}(\sqrt{t})$ for the classical random walk [2].

Due to these properties, the quantum random walk spreads quadratically faster than its classical counterpart. Quantum random walks are used in numerous different quantum algorithms to obtain quadratic or even exponential speed-ups, see for example [6,7,14].

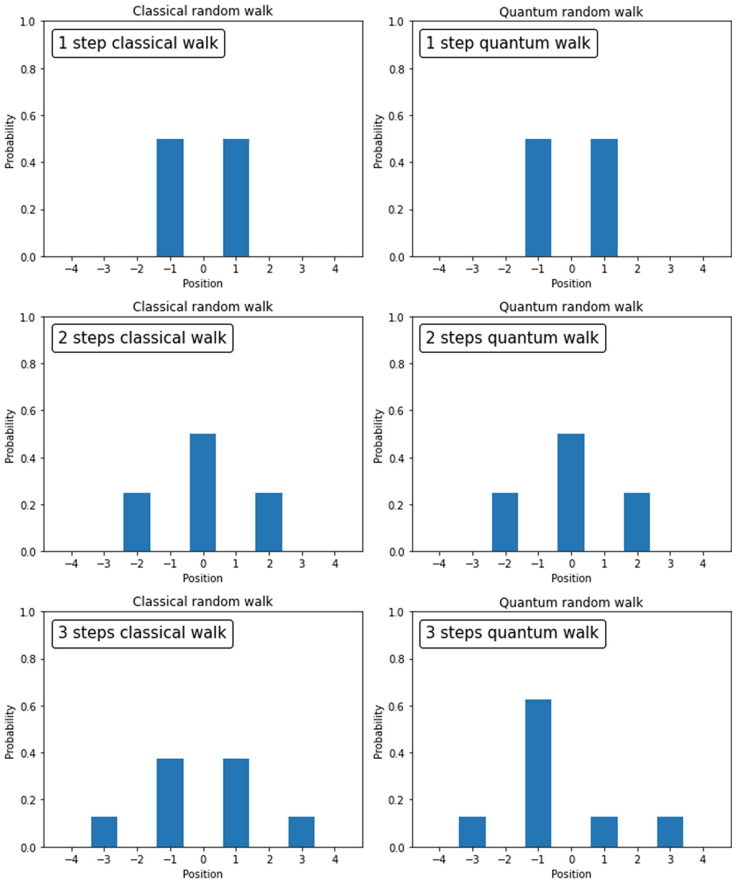

Fig. 7. Probability Distribution for First Steps of a Classical and a Quantum Random Walk

A.2 Quantum Walk in Two Dimensions

In this section we generalize the 1-dimensional quantum random walk to two dimensions based on the work of [3].

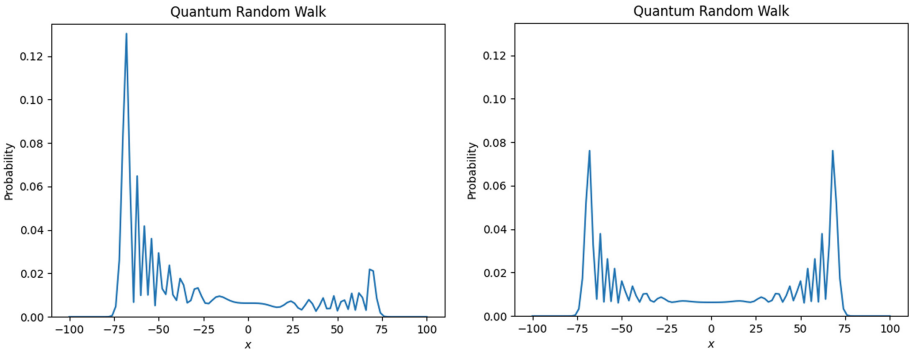

Fig. 8. Two Different Quantum Random Walks for the same Hadamard Coin Operator but Starting from a Different Initial Superposition. The Initial Superposition $\frac{1}{2}\sqrt{2}\,|0\rangle \otimes (|0\rangle + |1\rangle)$ (Left) Versus the Initial Superposition $\frac{1}{2}\sqrt{2}\,|0\rangle \otimes (|0\rangle + i\,|1\rangle)$ (right).

An agent at the position (x, y) on the two dimensional grid can be represented by a state $(|x\rangle \otimes |y\rangle) \otimes (|c_1\rangle \otimes |c_2\rangle)$ in $\mathbb{Z}^2 \times \text{span}\{|0\rangle, |1\rangle\}^2$, where the $|c_i\rangle$ are the coin-states. We define the two-dimensional quantum random walk to consist of the following two unitary operations

1. First apply what is known as the coin-flip operator $C = C_1 \otimes C_2$

$$C\left((|x\rangle \otimes |y\rangle) \otimes (|c_1\rangle \otimes |c_2\rangle)\right) = (|x\rangle \otimes |y\rangle) \otimes (C_1\,|c_1\rangle \otimes C_2\,|c_2\rangle)$$

2. Followed by the shift operator S

$$\begin{aligned}
S\left((|x\rangle \otimes |y\rangle) \otimes (|0\rangle \otimes |0\rangle)\right) &= (|x+1\rangle \otimes |y\rangle) \otimes (|0\rangle \otimes |0\rangle) \\
S\left((|x\rangle \otimes |y\rangle) \otimes (|0\rangle \otimes |1\rangle)\right) &= (|x-1\rangle \otimes |y\rangle) \otimes (|0\rangle \otimes |1\rangle) \\
S\left((|x\rangle \otimes |y\rangle) \otimes (|1\rangle \otimes |0\rangle)\right) &= (|x\rangle \otimes |y+1\rangle) \otimes (|1\rangle \otimes |0\rangle) \\
S\left((|x\rangle \otimes |y\rangle) \otimes (|1\rangle \otimes |1\rangle)\right) &= (|x\rangle \otimes |y-1\rangle) \otimes (|1\rangle \otimes |1\rangle)
\end{aligned}$$

A single step of the two-dimensional quantum walk is given by the application of S and C. Note that there is now even more freedom in the choice of the coin operator C, which can be any tensor product of two 2-dimensional unitary transformation matrix, resulting in many different families of the two dimensional quantum random walk. In [3] the limiting sets and other properties are studied for three different types of coin operators. Like in the case of the 1-dimensional quantum random walk, also the 2-dimensional quantum random walk is likely to have a bias towards certain directions, based on the coin operators and the initial state of the coin operator. It is however non-trivial to set the initial position to obtain a symmetric distribution, given a coin operator. As our goal is to make comparisons to symmetric random walks, performed on a symmetric grid, we do desire a symmetric walk. To obtain this we averaged four different quantum random walks to obtain a symmetric random walk. We call the resulting distribution the quantum-inspired random walk distribution, and is constructed as follows:

1. Choose a coin-flip operator, we chose:

$$C = (\mathbb{I}_2 \otimes \mathbb{I}_2) \otimes \frac{1}{2} \begin{pmatrix} 1 & -1 & -1 & -1 \\ -1 & 1 & -1 & -1 \\ -1 & -1 & 1 & -1 \\ -1 & -1 & -1 & 1 \end{pmatrix}.$$

2. Perform the N-step two-dimensional quantum random walk for the four initial states $(|0\rangle \otimes |0\rangle) \otimes (|i\rangle \otimes |j\rangle)$ with $i, j \in \{0, 1\}$.
3. Average the obtained probability distributions to obtain a symmetric distribution, see Fig. 9.

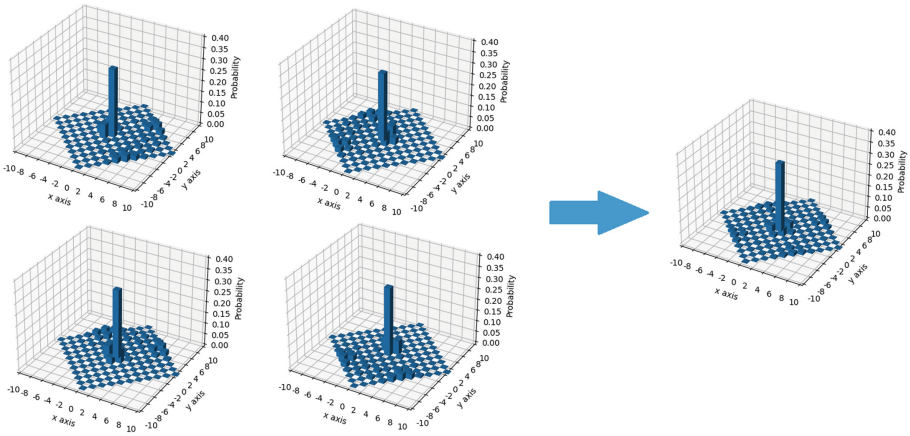

Fig. 9. The Four 10-Step Quantum Random Walks that are Combined with Equal Weights to Obtain the Quantum-Inspired Random Walk

References

1. Adams, E.S.: Boundary disputes in the territorial ant azteca trigona: effects of asymmetries in colony size. Anim. Behav. **39**(2), 321–328 (1990)
2. Ambainis, A.: Quantum walks and their algorithmic applications. Int. J. Quantum Inf., 1 (2004)
3. Baryshnikov, Y., Brady, W., Bressler, A., Pemantle, R.: Two-dimensional quantum random walk (2010)
4. Bonabeau, E.: Agent-based modeling: methods and techniques for simulating human systems. Proc. National Acad. Sci. **99**, 7280–7287 (2002)
5. Campanile, L., Gribaudo, M., Iacono, M., Mastroianni, M.: Hybrid simulation of energy management in IoT edge computing surveillance systems. In: Ballarini, P., Castel, H., Dimitriou, I., Iacono, M., Phung-Duc, T., Walraevens, J. (eds.) EPEW/ASMTA -2021. LNCS, vol. 13104, pp. 345–359. Springer, Cham (2021). https://doi.org/10.1007/978-3-030-91825-5_21

6. Chakraborty, S., Luh, K., Roland, J.: On analog quantum algorithms for the mixing of markov chains. ArXiv abs/1904.11895 (2019)
7. Childs, A., Cleve, R., Deotto, E., Farhi, E., Gutmann, S., Spielman, D.: Exponential algorithmic speedup by quantum walk. In: Conference Proceedings of the Annual ACM Symposium on Theory of Computing (2003)
8. Gordon, D.M.: Interaction patterns and task allocation in ant colonies, pp. 51–67. Birkhäuser Basel, Basel (1999)
9. Gordon, D.M., Paul, R.E., Thorpe, K.: What is the function of encounter patterns in ant colonies? Anim. Behav. **45**(6), 1083–1100 (1993)
10. Mahadik, K., Wu, Q., Li, S., Sabne, A.: Fast distributed bandits for online recommendation systems. In: ICS '20. Association for Computing Machinery (2020)
11. Musco, C., Su, H.-H., Lynch, N.A.: Ant-inspired density estimation via random walks. CoRR abs/1603.02981 (2016)
12. Pratt, S.C.: Quorum sensing by encounter rates in the ant Temnothorax albipennis. Behav. Ecol. **16**(2), 488–496 (2005)
13. Schafer, R.J., Holmes, S., Gordon, D.M.: Forager activation and food availability in harvester ants. Anim. Behav. **71**(4), 815–822 (2006)
14. Szegedy, M.: Quantum speed-up of markov chain based algorithms. In: 45th Annual IEEE Symposium on Foundations of Computer Science, pp. 32–41 (2004)